Gradient GPC for Optogenetics

Glückstad, Jesper

Publication date:
2013

Gradient GPC

An optical system for GPC-based image construction is schematized below. A phase modulated light beam is decomposed into Fourier components using a lens. A small, non-absorbing wave-retarder or phase contrast filter (PCF) at the center of the Fourier plane shifts the phase of the lowest spatial frequencies relative to the higher frequency components. Interference between frequency components upon recombination by a second lens creates the desired intensity distribution.

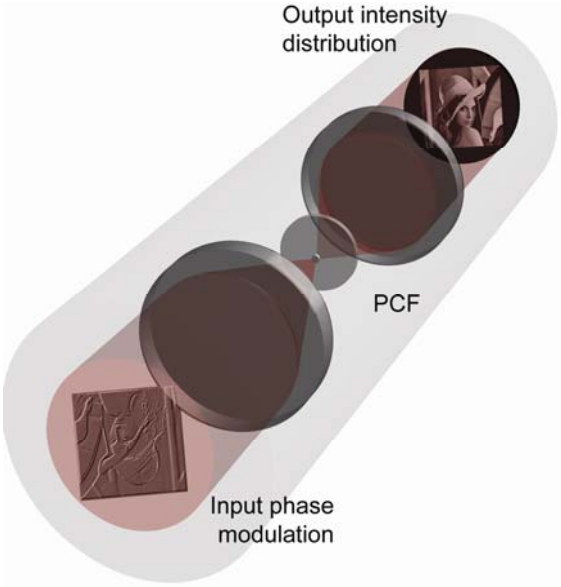

***Fig**. 1. Gradient GPC grey scale image mapping setup*

The optical field, $o(x,y)$, at the output plane of a GPC system can be described by a simple interference between two terms:

$$o(x,y)=\exp\left[\mathrm{i}\phi(x,y)\right]+c(x,y)\left[\exp(\mathrm{i}\theta)-1\right], \qquad (1)$$

where $\phi(x,y)$ is the phase distribution at the modulator and $c(x,y)$ describes a synthetic reference wave profile determined from Fourier components that have propagated through the phase-shifting region of the PCF with phase shift θ. If all AC components of $\exp\left[\mathrm{i}\phi(x,y)\right]$ fall outside the PCF at the Fourier plane, the approximation $c(x,y)\approx\bar{\alpha}\,g(x,y)$ is appropriate. $\bar{\alpha}$ is the complex-valued spatial average of the input field, and $g(x,y)$ is a real-valued function describing the composite diffractive effects due to the modulator and PCF hard-edge apertures.

Phasor diagrams are an intuitive way of analyzing light propagation in the GPC system. The three terms in Eq. (1) are represented by phasors **O**, **P**, and **R**, respectively (see Fig. 2). **P** is a unit phasor depicting the complex field at a single point on the modulator, and $\bar{\alpha}$ is the average of all **P** at the modulator plane. The identity: $\exp(\mathrm{i}\theta)-1=2\left|\sin(\theta/2)\right|\exp\left[\mathrm{i}(\theta+\pi)/2\right]$, shows that the reference wave, **R** is always angularly displaced from $\bar{\alpha}$ by $(\theta+\pi)/2$. The output field, **O**, is then constructed simply by taking the sum of each **P** with **R**. For any particular **P**, its complex conjugate, **P'**, with respect to **R** will yield the same output intensity.

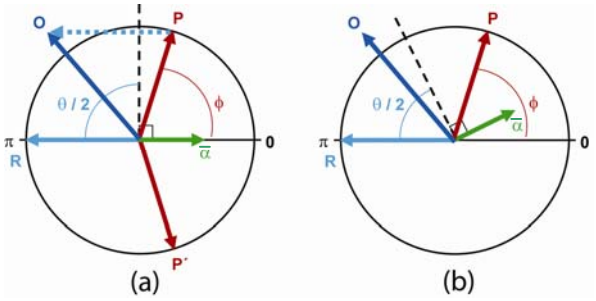

Fig. 2. *Phasor diagrams of interfering light components in a GPC system. (a) Alternate-pixel conjugation scheme with $\theta = \pi$. (b) Arbitrary scheme requiring only 0 to π encoding.*

In the next section, we will show how to utilize this degeneracy in a phase conjugation scheme for constructing arbitrary grey-level images, which can be understood from Fig. 2(a). The aim is to position the phase of $\bar{\alpha}$ and **R** to 0 and π, respectively, by alternately conjugating pixels in a slowly varying phase pattern and choosing a PCF with $\theta = \pi$. If the PCF size is appropriately chosen such that $g(0,0) = 1$, the output image follows the simple mapping:

$$\left|o(x,y)\right|^2 = 4\left|\sin\left[\phi(x,y)/2\right]\right|^2. \qquad (3)$$

Although Eq. (3) neglects a slight modulation envelope in $g(x,y)$ that causes a decrease in contrast towards the outer edges of the image, very good image quality with up to four-fold gain in peak intensity is still achievable. Implementing a phase-conjugation scheme requires an SLM device with very good modulation transfer function (MTF) to properly render rapidly varying phase between adjacent pixels. It also requires consistent phase encoding performance over a complete 2π phase stroke.

The phasor diagram in Fig. 2(b) depicts an alternative encoding scheme that works for most available devices, which are characterized by a moderate MTF. Rather than forcing the phase of $\bar{\alpha}$ to 0 through phase-conjugation, **R** can be independently brought to π by matching θ to the existing $\bar{\alpha}$. The output intensity will still map according to Eq. (3), but without the need for encoding conjugate phases. Thus, both MTF and phase stroke requirements on the implementing device are greatly relaxed. The reduced phase stroke requirement is particularly significant as it would allow the adoption of faster SLM devices. We note, however, that $\bar{\alpha}$ is image dependent, *i.e.* it varies with the histogram of the encoded phase pattern. An ideal system should then utilize a dynamic PCF whose phase shift can be adjusted as arbitrary images are introduced to the projection system.

A similar projection scheme may also be applied with a fixed PCF if a dynamic filter is not available. Instead of adjusting the phase shift, the histogram of the encoded pattern may be modified such that the correct phase for $\bar{\alpha}$ and consequently for **R**, is achieved. In particular, histogram equalization ensures that the average phase is consistent and independent of any specific image information. The principal image can then be circumscribed with a frame of zero-phase pixels to shift the effective $\bar{\alpha}$ to a smaller phase value. To find the optimal frame size, we must apply the design criterion that relates $\bar{\alpha}$ and PCF shift, θ. The optimum fill-factor, F, of the principal image with respect to the entire illuminated area is then derived from the complex-valued expression

$$\bar{\alpha}' = \frac{1 - 2(1-F)\,g(0,0) + \mathrm{i}\cot\left(\theta/2\right)}{2Fg(0,0)}, \qquad (4)$$

where $\bar{\alpha}'$ indicates the complex spatial average of the principal image before the zero-phase frame is applied.

This framing technique allows the $\bar{\alpha}$ of different framed grey-level images to be consistently matched to a fixed PCF with arbitrary θ. Equation (4) ensures that we satisfy the condition depicted in Fig. 2(b), where the zero-padding frame appears dark at the output plane and energy is diverted almost entirely into the central region containing the principal image.

In comparison to previously known phase-only imaging techniques this dramatically simplifies the synthesis of arbitrary intensity patterns and the requirements of the space bandwidth product are also significantly reduced compared to that of e.g. phase-only holography. This makes it more feasible to utilize a dynamic and relatively coarse grained spatial light modulator as input phase modulating device without seriously compromising on the image reconstruction quality. The experimental demonstration of laser image projection was implemented using a typical GPC imaging system. A telescopic lens pair (f = 35 mm, f = 1000 mm) expanded the 830-nm output from a Ti:Sapphire laser (Spectra Physics 3900) to illuminate a reflection-type optically-addressed phase-only SLM (Hamamatsu PPM X7550, 41.6 μm/pixel) through a circular aperture (diameter = 11.5 mm). The SLM is at the front focal plane of a standard 4*f* imaging setup (f1 = 300 mm, f2 = 150 mm) with a CCD camera (Pulnix TM-765, 11 μm/pixel) located at the back focal plane of the second lens. A phase contrast filter (PCF) sits at the confocal plane between the two lenses. The PCF consists of a circular pit (diameter = 33 μm) etched on an optical flat. The pit is aligned at the optical axis and provides θ~2 radians phase shift between the zero-order and the higher order Fourier components.

Fig. 3(a) presents the intensity distribution captured by a CCD at the output image plane of the GPC system. The projected image is an excerpt from the well-known "Lena" image. Figure 3(b) shows the output of the system when the PCF is removed from the optical train. In an ideal system, phase-only modulation implies that this image should be of uniform intensity. It is obvious, however, that some amplitude modulation has been introduced by the SLM and other optical components.

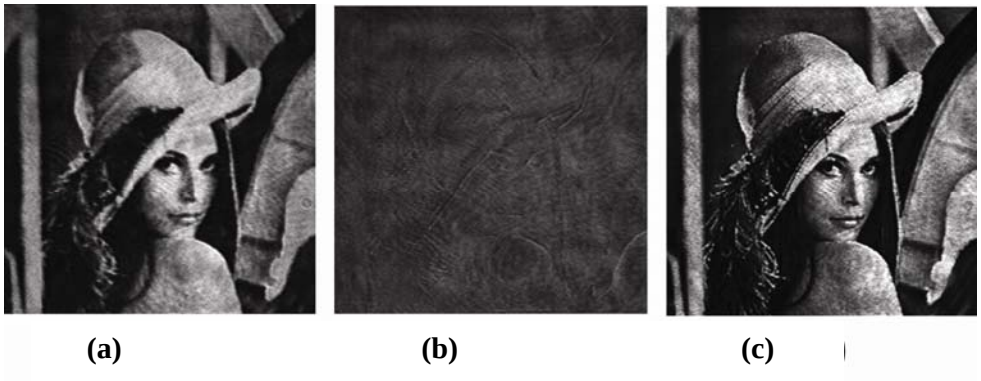

Fig. 3*. Image projection of a GPC system. (a) Image captured with a CCD at the output plane. (b) Intensity distribution at the output plane when the PCF is removed. (c) Numerically simulated image projection incorporating amplitude modulation crosstalk.*

A simulated projection taking into consideration such crosstalk was numerically calculated and is shown in Fig. 3(c). Most of the observable intensity artifacts in the captured image are reproduced here. These errors are thus more indicative of device limitations and read-out beam quality, rather than fundamental limitations of the projection scheme. The principal difference between the simulated and actual projections is a softening of edge information. Such loss of high spatial frequency content is attributed to the limited MTF of the SLM, as well as the finite lens apertures in the Fourier lens system.